COMPUTATIONAL INVERSE MEDIUM SCATTERING AT FIXED FREQUENCY

Gang Bao* and Peijun Li†

Abstract

A continuation method is presented for solving the inverse medium scattering problem of the Helmholtz equation in $\mathbb{R}^2$. The algorithm requires only single-frequency scattering data. Using an initial guess from the Born approximation, each update is obtained via recursive linearization on the spatial frequency of a one-parameter family of plane waves by solving one forward and one adjoint problem of the Helmholtz equation.

1 Introduction

Consider the Helmholtz equation in two dimensions

$$\Delta\phi + k_0^2(1 + q(x))\phi = 0, \tag{1.1}$$

where ϕ is the total field, k_0 is the wavenumber, and $q(x) > -1$, which has a compact support, is the scatterer. The scatterer is illuminated by a one-parameter family of plane waves

$$\phi_0(x_1, x_2) = e^{i(\eta x_1 + k(\eta)x_2)},$$

where

$$k(\eta) = \begin{cases} \sqrt{k_0^2 - \eta^2} & \text{for } k_0 \geq |\eta|, \\ i\sqrt{\eta^2 - k_0^2} & \text{for } k_0 < |\eta|. \end{cases}$$

The number $|\eta|$ is the spatial frequency.

The modes for which $|\eta| \leq k_0$ correspond to propagating plane waves while the modes with $|\eta| > k_0$ correspond to evanescent plane waves, which may be generated at the interface of two media by total internal reflection [5, 9]. These waves are oscillatory parallel to the x_1 axis and decay exponentially along the x_2 axis in the upper half plane $\mathbb{R}_+^2 = \{(x_1, x_2) \in \mathbb{R}^2 : x_2 > 0\}$. Evidently, such incident waves satisfy the homogeneous equation

$$\Delta\phi_0 + k_0^2\phi_0 = 0. \tag{1.2}$$

The total electric field ϕ consists of the incident field ϕ_0 and the scattered field ψ:

$$\phi = \phi_0 + \psi.$$

It follows from the equations (1.1) and (1.2) that the scattered field satisfies

$$\Delta\psi + k_0^2(1+q)\psi = -k_0^2 q\phi_0. \tag{1.3}$$

Let D be a bounded domain in $\mathbb{R}^2$ with boundary ∂D, which contains the compact support of the scatterer $q(x)$. Denote n the unit outward normal to ∂D. For simplicity, we employ the first order absorbing boundary condition [11] as

$$\frac{\partial\psi}{\partial n} - \mathrm{i}k_0\psi = 0 \quad \text{on } \partial D, \tag{1.4}$$

The inverse medium scattering problem is to determine the scatterer $q(x)$ from the measurements of near-field currents densities, $\psi|_{\partial D}$, given the incident field ϕ_0. The inverse medium scattering problems arise naturally in diverse applications such as radar, sonar, geophysical exploration, medical imaging, and nondestructive testing [8]. There are two major difficulties associated with these inverse problems: the ill-posedness and the presence of many local minima. In this paper, we present an algorithm which overcomes the difficulties. Our algorithm requires single-frequency scattering data and the recursive linearization is obtained by a continuation method on the spatial frequency. It first solves a linear integral equation (Born approximation) at the largest spatial frequency. Updates are made by using the data at smaller spatial frequency sequentially. For each iteration, one forward and one adjoint problem of Helmholtz equation are solved. Two new computational examples are presented. We refer the reader to [4] for a complete description of the algorithm and related analysis. See also [2, 3, 6, 7] for related stable and efficient continuation methods for solveing the two-dimensional Helmholtz equation and the three-dimensional Maxwell's equations in the case of full aperture data. A homotopy continuation method with limited aperture data may be found in [1].

2   Born approximation

Rewrite (1.3) as

$$\Delta\psi + k_0^2\psi = -k_0^2 q(\phi_0 + \psi). \tag{2.1}$$

Consider a test function $\psi_0 = e^{\mathrm{i}k_0 x \cdot \vec{d}}, \vec{d} = (\cos\theta, \sin\theta), \theta \in [0, 2\pi]$. Hence ψ_0 satisfies (1.2).

Multiplying the equation (2.1) by ψ_0, and integrating over D on both sides, we have

$$\int_D \psi_0 \Delta\psi dx + k_0^2 \int_D \psi_0\psi dx = -k_0^2 \int_D q(\phi_0 + \psi)\psi_0 dx.$$

Integration by parts yields

$$\int_D \psi\Delta\psi_0 dx + \int_{\partial D}\left(\psi_0\frac{\partial\psi}{\partial n} - \psi\frac{\partial\psi_0}{\partial n}\right)ds + k_0^2 \int_D \psi_0\psi dx = -k_0^2 \int_D q(\phi_0 + \psi)\psi_0 dx.$$

We have by noting (1.2) and the boundary condition (1.4) that

$$\int_D q(\phi_0 + \psi)\psi_0 dx = \frac{1}{k_0^2}\int_{\partial D} \psi\left(\frac{\partial\psi_0}{\partial n} - \mathrm{i}k_0\psi_0\right)ds.$$

2

Using the special form of the incident wave and the test function, we then get

$$\int_D q(x)e^{i(\eta + k_0 \cos\theta)x_1}e^{i(k(\eta)+k_0 \sin\theta)x_2}dx = \frac{i}{k_0}\int_{\partial D}\psi(n\cdot\vec{d}-1)e^{ik_0 x\cdot\vec{d}}ds - \int_D q\psi\psi_0 dx. \qquad (2.2)$$

When the spatial frequency $|\eta|$ is large, the scattered field is weak and the inverse scattering problem becomes essentially linear. See [4] for an energy estimate of the scattered field. Dropping the nonlinear (second) term of (2.2), we obtain the linearized integral equation

$$\int_D q(x)e^{i(\eta + k_0 \cos\theta)x_1}e^{(-\sqrt{\eta^2-k_0^2}+ik_0 \sin\theta)x_2}dx = \frac{i}{k_0}\int_{\partial D}\psi(n\cdot\vec{d}-1)e^{ik_0 x\cdot\vec{d}}ds, \qquad (2.3)$$

which is the Born approximation. In practice, the integral equation (2.3) is implemented by using Landweber iteration in order to reduce the computational cost and instability [10, 13].

When a medium is probed with an evanescent plane wave at a high spatial frequency, only a thin layer of the medium is penetrated. Corresponding to this exponentially decaying incident field, the scattered field measured on the boundary contains information of the medium in that thin layer. To accurately determine the medium, information at lower spatial frequencies of the evanescent plane waves is needed to illuminate the medium.

3 Recursive linearization

As discussed in the previous section, when the spatial frequency $|\eta|$ is large, the Born approximation allows a reconstruction of the thin layer for the true scatterer. Choose a large positive number η_{max} and divide the interval $[0, \eta_{max}]$ into N subdivisions with the endpoints $\{\eta_0, \eta_1, ..., \eta_N\}$, where $\eta_0 = 0, \eta_N = \eta_{max}$, and $\eta_{i-1} < \eta_i$ for $1 \le i \le N$. We now describe a procedure that recursively determines q_η at $\eta = \eta_N, \eta_{N-1}, ..., \eta_0$.

Suppose now that the scatterer $q_{\tilde{\eta}}$ has been recovered at some $\tilde{\eta} = \eta_{i+1}$ and that $\eta = \eta_i$ is slightly less than $\tilde{\eta}$. We wish to determine q_η, or equivalently, to determine the perturbation

$$\delta q = q_\eta - q_{\tilde{\eta}}.$$

For the reconstructed scatterer $q_{\tilde{\eta}}$, we solve at the spatial frequency η the forward scattering problem

$$\Delta\tilde{\psi}^{(j,i)} + k_0^2(1+q_{\tilde{\eta}})\tilde{\psi}^{(j,i)} = -k_0^2 q_{\tilde{\eta}}\phi_0^{(j,i)}, \qquad (3.1)$$

$$\frac{\partial\tilde{\psi}^{(j,i)}}{\partial n} - ik_0\tilde{\psi}^{(j,i)} = 0, \qquad (3.2)$$

where the incident wave $\phi_0^{(j,i)} = e^{i\eta_j x_1 + ik(\eta_j)x_2}, |j| \ge i$.

For the scatterer q_η, we have

$$\Delta\psi^{(j,i)} + k_0^2(1+q_\eta)\psi^{(j,i)} = -k_0^2 q_\eta\phi_0^{(j,i)}, \qquad (3.3)$$

$$\frac{\partial\psi^{(j,i)}}{\partial n} - ik_0\psi^{(j,i)} = 0. \qquad (3.4)$$

Subtracting (3.1), (3.2) from (3.3), (3.4) and omitting the second-order smallness in δq and in $\delta \psi^{(j)} = \psi^{(j,i)} - \tilde{\psi}^{(j,i)}$, we obtain

$$\Delta \delta \psi^{(j)} + k_0^2 (1 + q_{\tilde{\eta}}) \delta \psi^{(j)} = -k_0^2 \delta q (\phi_0^{(j,i)} + \tilde{\psi}^{(j,i)}), \tag{3.5}$$

$$\frac{\partial \delta \psi^{(j)}}{\partial n} - \mathrm{i} k_0 \delta \psi^{(j)} = 0. \tag{3.6}$$

For the scatterer q_η and the incident wave $\phi_0^{(j,i)}$, we define the map $S_j(q_\eta, \phi_0^{(j,i)})$ by

$$S_j(q_\eta, \phi_0^{(j,i)}) = \psi^{(j,i)},$$

where $\psi^{(j,i)}$ is the scattering data corresponding to the incident wave $\phi_0^{(j,i)}$. Let γ be the trace operator to the boundary ∂D. Define the scattering map

$$M_j(q_\eta, \phi_0^{(j,i)}) = \gamma S_j(q_\eta, \phi_0^{(j,i)}).$$

For simplicity, denote $M_j(q_\eta, \phi_0^{(j,i)})$ by $M_j(q_\eta)$. By the definition of the trace operator, we have

$$M_j(q_\eta) = \psi^{(j,i)}|_{\partial D}.$$

Let $DM_j(q_{\tilde{\eta}})$ be the Fréchet derivative of $M_j(q_\eta)$ and denote the residual operator by

$$R_j(q_{\tilde{\eta}}) = \psi^{(j,i)}|_{\partial D} - \tilde{\psi}^{(j,i)}|_{\partial D}.$$

It follows from [4] that

$$DM_j(q_{\tilde{\eta}}) \delta q = R_j(q_{\tilde{\eta}}). \tag{3.7}$$

Similarly, in order to reduce the computation cost and instability, we consider the Landweber iteration of (3.7), which has the form

$$\delta q = \beta DM_j^*(q_{\tilde{\eta}}) R_j(q_{\tilde{\eta}}) \quad \text{for all } |j| \geq i, \tag{3.8}$$

where β is a relaxation parameter and $DM_j^*(q_{\tilde{\eta}})$ is the adjoint operator of $DM_j(q_{\tilde{\eta}})$.

In order to compute the correction δq, we need some efficient way to compute $DM_j^*(q_{\tilde{\eta}}) R_j(q_{\tilde{\eta}})$, which is given by the following theorem. See [4] for the proof.

Theorem 3.1. *Given residual $R_j(q_{\tilde{\eta}})$, there exits a function $\phi^{(j,i)}$ such that the adjoint Fréchet derivative $DM_j^*(q_{\tilde{\eta}})$ satisfies*

$$\left[DM_j^*(q_{\tilde{\eta}}) R_j(q_{\tilde{\eta}}) \right](x) = k_0^2 \left(\overline{\phi_0^{(j,i)}}(x) + \overline{\tilde{\psi}^{(j,i)}}(x) \right) \phi^{(j,i)}(x), \tag{3.9}$$

where $\phi_0^{(j,i)}$ is the incident wave and $\tilde{\psi}^{(j,i)}$ is the solution of (3.1), (3.2) with the incident wave $\phi_0^{(j,i)}$.

Using this theorem, we can rewrite (3.8) as

$$\delta q = k_0^2 \beta \left(\overline{\phi_0^{(j,i)}} + \overline{\tilde{\psi}^{(j,i)}} \right) \phi^{(j,i)}. \tag{3.10}$$

So for each incident wave with a transverse part η_j, we have to solve one forward problem along with one adjoint problem for the Helmhotlz equation. Since the adjoint problem has a similar variational form as the forward problem. Essentially, we need to compute two forward problems at each sweep. Once δq is determined, $q_{\tilde{\eta}}$ is updated by $q_{\tilde{\eta}} + \delta q$. After completing sweeps with $|\eta_j| \geq \eta$, we get the reconstructed scatterer q_η at the spatial frequency η.

4 Numerical experiments

In this section, we present two numerical examples to illustrate the performance of the algorithm. For test of stability, some relative random noise is added to the data, i.e. the electric field takes the form

$$\psi|_{\partial D} := (1 + \sigma \, \text{rand})\psi|_{\partial D}.$$

Here, rand gives uniformly distributed random numbers in $[-1, 1]$ and σ is a noise level parameter taken to be 0.02 in our numerical experiments. The relaxation parameter β is taken to be 0.01.

Example 1. Reconstruct a scatterer defined by

$$q_1(x_1, x_2) = \begin{cases} 2.0 & \text{for } r \le 0.6, \\ 0 & \text{for } r > 0.6, \end{cases}$$

inside the domain $D = [-1, 1] \times [0, 2]$, where $r = \sqrt{x_1^2 + (x_2 - 1)^2}$. See Figure 1 and Figure 2 for the surface and image views of the scatterer function. This example is used to examine the invalidity of Born approximation. In [12], the author derived an explicit error bound of the Born approximation for inverse scattering problem of the Helmholtz equation at fixed frequency. For the validity of the Born approximation, one needs a condition of the form

$$\rho k_0 \gamma(k_0) \sup_{|x| \le \rho} |q(x)| < 1,$$

where ρ is the radius of some region containing the compact support of the scatterer q, k_0 is the wavenumber, and γ is a positive constant, which depends on the wavenumber k_0. In the context of Example 1, these parameters are $\rho = 0.6$, $k_0 = 15.0$, $\gamma = 0.63$, and $\sup_{|x| \le \rho} |q(x)| = 2.0$. It follows from simple calculation that

$$\rho k_0 \gamma(k_0) \sup_{|x| \le \rho} |q(x)| = 11.34,$$

which is beyond the validity of Born approximation. Figure 3 gives the evolution of reconstruction horizontally across $x_2 = 1.0$. Due to the discontinuity of the given scatterer, the Gibbs phenomenon appears in the reconstructed scatterer.

Example 2. Reconstruct a scatterer defined by

$$q_2(x_1, x_2) = 0.5(1 + \cos(3\pi x_1))\sin(2.5\pi x_2)$$

inside the domain $D_2 = [-1, 1] \times [0, 0.4]$. This example is used to illustrate the resolution of the reconstruction using different wavenumbers. The x_1-transverse spatial frequency of q_2 is 3π, which accounts for the x_1-transverse wavelength about 0.67. Figure 4 shows the images of reconstructions using different wavenumbers k_0 at π, 1.5π, and 3π, corresponding to wavelengths of 2.0, 1.33, and 0.67, respectively. Figure 5 gives the slice of reconstructions at $x_2 = 0.2$ using different wavenumbers. Figure 4 and Figure 5 present the effect of the wavenumber k_0 on the result of reconstruction, which illustrates clearly that the inversion using a larger wavenumber k_0 is better than that using a smaller one. This result may be explained by Heisenberg's uncertainty principle [6, 7].
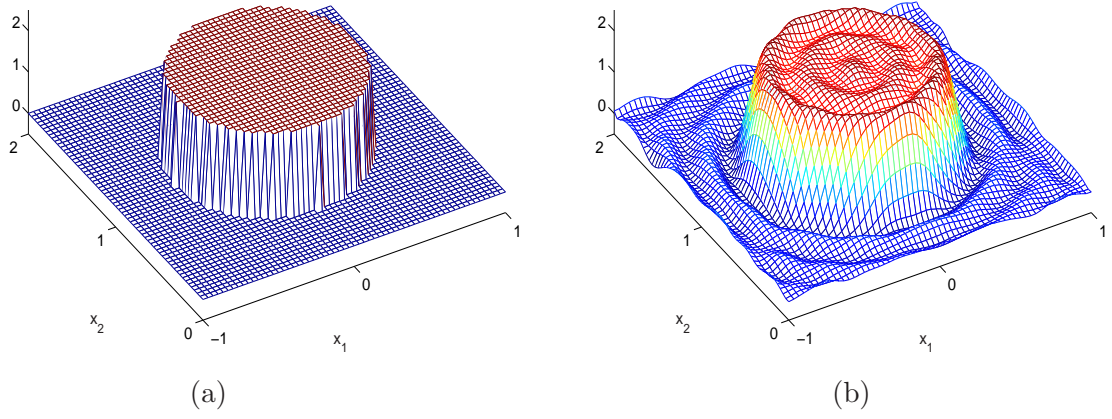
Figure 1: reconstruction of q_1. (a) true scatterer; (b) reconstruction.
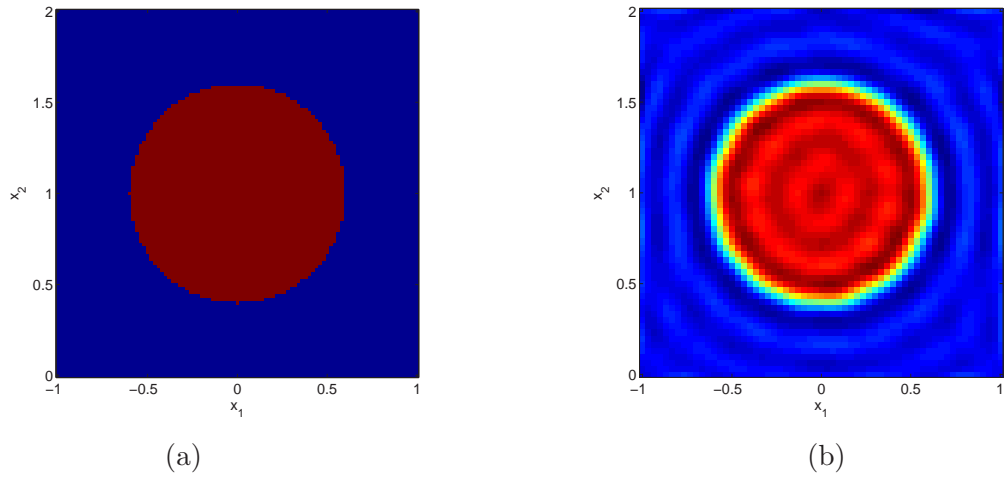
Figure 2: image of reconstruction for q_1. (a) true scatterer; (b) reconstruction.

6
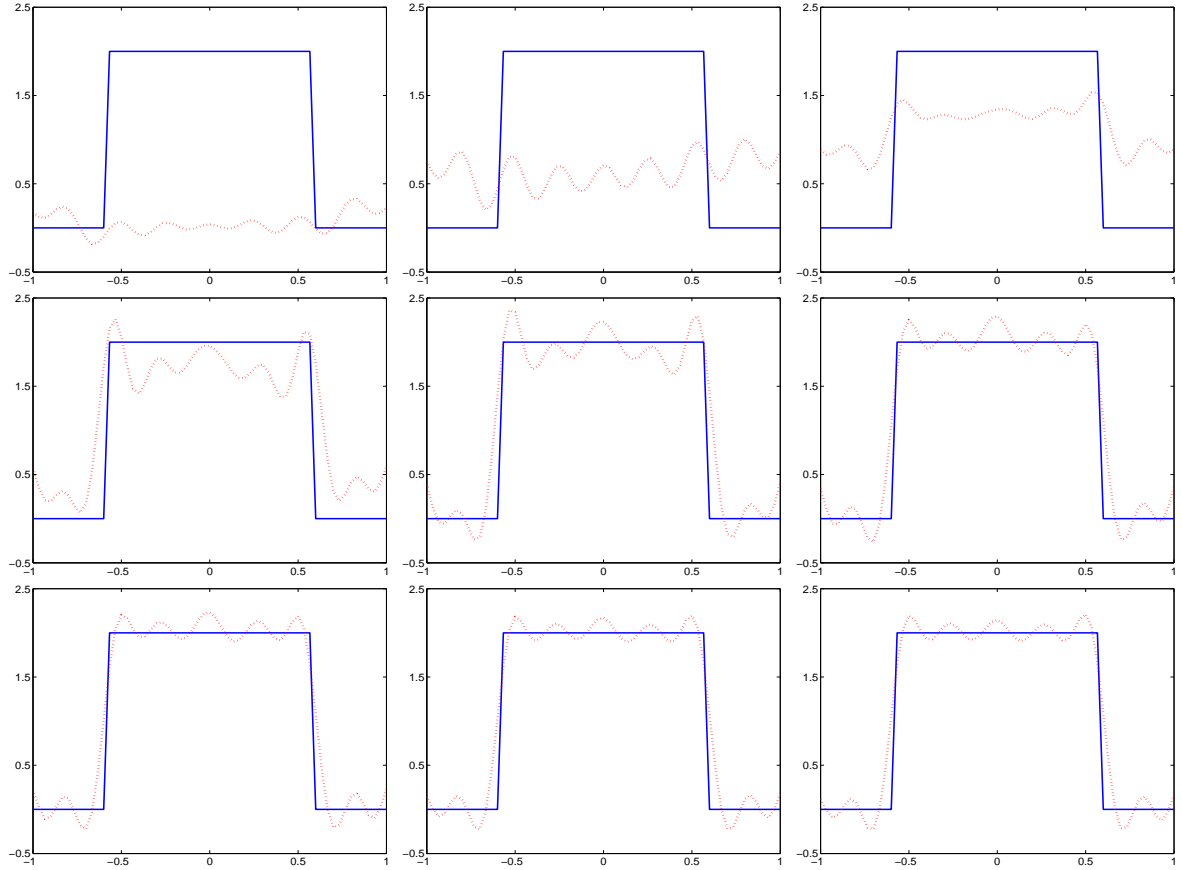
Figure 3: evolution of slice for the reconstruction q_1. Solid curve: true scatterer; dotted curve: reconstruction. Top row from left to right: reconstruction at $\eta = 14.45$; reconstruction at $\eta = 13.60$; reconstruction at $\eta = 12.75$; middle row from left to right: reconstruction at $\eta = 10.20$; reconstruction at $\eta = 8.50$; reconstruction at $\eta = 6.80$; bottom row from left to right: reconstruction at $\eta = 5.10$; reconstruction at $\eta = 2.55$; reconstruction at $\eta = 0.0$.
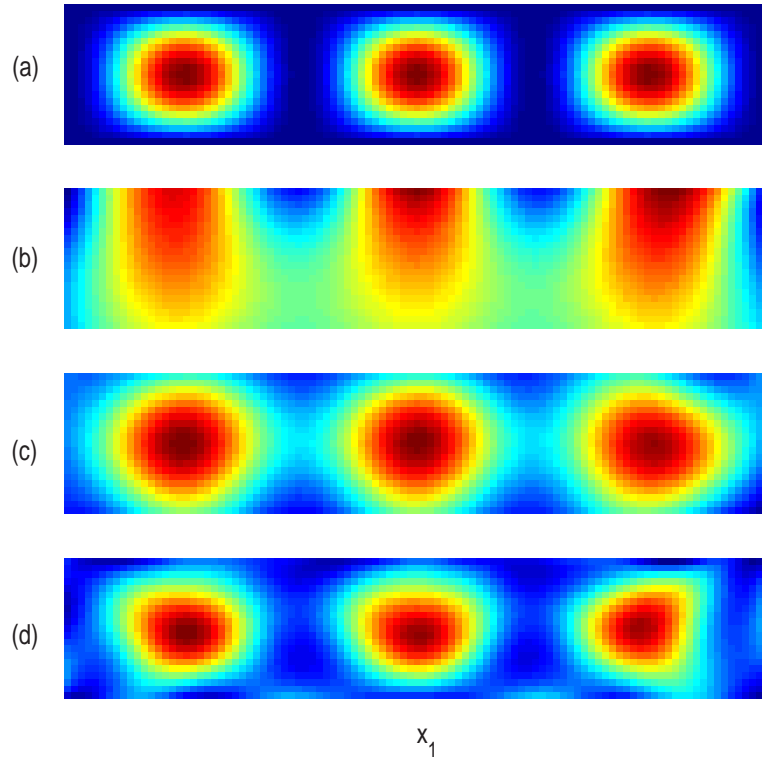
Figure 4: image views of reconstructions for q_2 with different wavenumbers. (a) true scatterer; (b) reconstruction using $k_0 = \pi$; (c) reconstruction using $k_0 = 1.5\pi$; (d) reconstruction using $k_0 = 3\pi$.
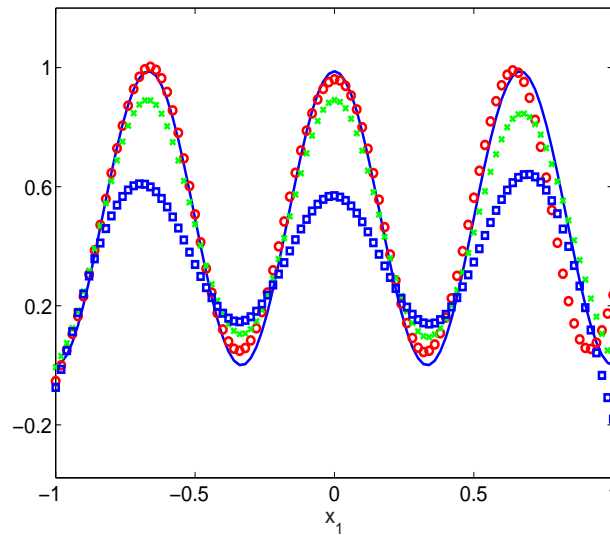
Figure 5: slice of reconstructions for q_2 with different wavenumbers. Solid curve: true scatterer; $\square$: reconstruction using $k_0 = \pi$; x: reconstruction using $k_0 = 1.5\pi$; $\circ$: reconstruction using $k_0 = 3\pi$.

5   Concluding remarks

We have presented a new continuation method with respect to the spatial frequency of a one-parameter family of plane waves. The recursive linearization algorithm is robust and efficient for solving the inverse medium scattering at fixed frequency. Finally, we point out some future directions along the line of this work. The first is concerned with the convergence analysis. Although our numerical experiments demonstrate the convergence and stability of the inversion algorithm, no rigorous mathematical result is available at present. Another important and interesting project is to investigate scattering problems in near-field optics since evanescent plane waves can only occur in the near-field zone. In the case of near-field optics, scattering problems are more appropriate to be formulated in the configuration of half-space instead of free space. We are currently attempting to extend the approach in this paper to more realistic models in the half-space geometry and will report the progress elsewhere.

References

[1] G. Bao and J. Liu, *Numerical solution of inverse problems with multi-experimental limited aperture data*, SIAM J. Sci. Comput., 25 (2003), pp. 1102–1117.

[2] G. Bao and P. Li, *Inverse medium scattering for three-dimensional time harmonic Maxwell equations*, Inverse Problems, 20 (2004), pp. L1–L7.

[3] G. Bao and P. Li, *Inverse medium scattering problems for electromagnetic waves*, SIAM J. Appl. Math., 65 (2005), pp. 2049–1066.

[4] G. Bao and P. Li, *Inverse medium scattering for the Helmholtz equation at fixed frequency*, Inverse Problems, 21 (2005), pp. 1621–1641.

[5] P. Carney and J. Schotland, *Three-dimensional total internal reflection microscopy*, Opt. Lett., 26 (2001), pp. 1072–1074.

[6] Y. Chen, *Inverse scattering via Heisenberg uncertainty principle*, Inverse Problems, 13 (1997), pp. 253–282.

[7] Y. Chen, *Inverse scattering via skin effect*, Inverse Problems, 13 (1997), pp. 649–667.

[8] D. Colton and R. Kress, *Inverse Acoustic and Electromagnetic Scattering Theory*, 2nd ed., Appl. Math. Sci. 93, Springer-Verlag, Berlin, 1998.

[9] D. Courjon, *Near-field Microscopy and Near-field Optics*, Imperial College Press, 2003.

[10] H. Engl, M. Hanke, and A. Neubauer, *Regularization of Inverse Problems*, Dordrecht: Kluwer, 1996.

[11] J. Jin, *The Finite Element Methods in Electromagnetics*, John Wiley & Sons, 2002.

[12] F. Natterer, *An error bound for the Born approximation*, Inverse Problems, 20 (2004), pp. 447–452.

[13] F. Natterer, *The Mathematics of Computerized Tomography*, Stuttgart: Teubner, 1986.